Check for updates

From açaí (*Euterpe oleracea* Mart.) waste to mannose and mannanoligosaccharides: a one-step process for recalcitrant mannan depolymerization using dilute oxalic acid†

Fernanda Thimoteo Azevedo Jorge, [ID] [a] Ingrid Santos Miguez, [ID] [a,b] George Victor Brigagão [ID] [c] and Ayla Sant'Ana da Silva [ID] *[a,b]

Açaí seeds are an abundant agroindustrial residue from the Brazilian Amazon region and comprise a rich source of linear mannan polysaccharide, which offers high potential for valorization into bioactive mannose and mannanoligosaccharides. This work optimizes mannose production from açaí seeds using dilute oxalic acid as a safer and greener alternative to sulfuric acid. Experiments were performed to analyze the effects of hydrolysis temperature, time and acid concentration, achieving a maximum mannose yield of 83% when employing 6.0% w/w oxalic acid at 177 °C for 15 min. This is the highest mannose yield ever reported for a one-step hydrolysis of recalcitrant linear mannan using an organic acid. In addition to mannose, this process coproduces mannanoligosaccharides in 9.6% yield. Furthermore, the economic viability of this novel process is demonstrated on an industrial scale *via* process simulation and techno-economic analysis of a biorefinery processing 6000 kg h^{-1} of açaí seeds. The simulated process considered oxalic acid recovery and recycling by chromatography, avoiding the use of a base for hydrolysate neutralization and the generation of salt waste, thus minimizing the environmental impacts of the process. The techno-economic analysis revealed a high profitability for a mannose selling price of US$ 10 per kg, resulting in a net present value of US$ 188 million and a payback period of 2.5 years after startup. Therefore, this work provides significant advances in mannose production, offering an efficient and economically viable one-step hydrolysis process that reduces waste, uses renewable raw materials and less harmful chemicals, and has the potential to contribute to a circular bioeconomy in the Amazon region.

1. Introduction

The transition towards a sustainable economy requires the development of green, efficient and cost-effective biorefinery systems to produce biofuels, chemicals, and electricity from renewable biobased resources.[1] To achieve this goal, agricultural wastes play an important role as feedstocks with large and decentralized availability across different regions and countries, which can be converted into multiple value-added products and promote a circular bioeconomy.[2] Nevertheless,

challenges still remain in deconstructing their complex plant cell wall structure and achieving high conversions in a green and cost-effective way.[3,4]

In the context of the Brazilian Amazon region, açaí (*Euterpe oleracea* Mart.) seeds stand out as a large-scale waste that could be valorized in a biorefinery.[5,6] The açaí fruit has high socioeconomic relevance for local communities and it is the most commercially successful Amazonian product worldwide,[7] with an annual production exceeding 1.2 million tons since 2015 and reaching 1.9 million tons in 2023.[8] However, the edible açaí pulp corresponds to only ~15% of the fruit weight, while the remaining 85% corresponds to a seed that is regarded as waste.[9] Currently, açaí seeds are seldom valorized and their applications comprise mainly low added-value products, such as organic compost, heat and electricity.[10] Still, large amounts of seeds remain unutilized and are often disposed of in open dumps, water bodies, and sanitary landfills, entailing severe environmental and sanitary problems.[6]

Despite their current disposal as waste, açaí seeds display a valuable chemical composition that enables their conversion

[a]Laboratório de Biocatálise, Instituto Nacional de Tecnologia, Ministério da Ciência, Tecnologia e Inovações, Rio de Janeiro, 20081-312 RJ, Brazil. E-mail: ayla.santana@int.gov.br

[b]Departamento de Bioquímica, Instituto de Química, Universidade Federal do Rio de Janeiro, Rio de Janeiro, 21941-909 RJ, Brazil

[c]Departamento de Engenharia Industrial, Escola Politécnica, Universidade Federal do Rio de Janeiro, Rio de Janeiro, 21941-909 RJ, Brazil

†Electronic supplementary information (ESI) available. See DOI: https://doi.org/10.1039/d4gc03732d

into high-value products. The seeds' bioactive polyphenolic compounds have led to growing interest in obtaining açaí seed extracts, which display beneficial pharmacological properties.[11,12] Besides, açaí seeds are a rich source of mannan, a polysaccharide composed of mannose units that corresponds to 45–55% of the total dry weight of the seed, a content considerably higher than those of other agro-industrial wastes.[5,13,14] In addition, the suggested structure of açaí seeds' mannan is linear with a low degree of substitution,[13] which makes açaí seeds a promising source of mannose and mannanoligosaccharides (MOS) with high mass yield and purity.

Mannose is a bioactive monosaccharide of great interest for several industrial sectors. It is mainly commercialized for the treatment and prevention of urinary tract infections,[15,16] besides being used in the food industry as a texturizer[16] and in cosmetic formulations as a humectant.[17] However, its limited availability and high cost compared to other sugars restrict its potential use as a raw material for producing other substances, which highlights the need for more efficient and cost-effective processes to produce mannose on a larger scale.[13,16] Besides mannose, MOS (oligosaccharides with 2 to 10 mannose units) can be coproduced from mannan hydrolysis, enabling additional market applications due to their prebiotic function and well-established commercial use as animal feed additives.[18,19]

Nevertheless, the hydrolysis of açaí seeds into mannose and MOS presents a technical challenge due to its mannan structure, which is crystalline and highly insoluble in water.[13] Unlike other plant-derived heteropolymeric amorphous mannans, such as galactomannans and yeast-derived α-mannans, hydrolyzing crystalline mannan typically requires severe conditions using corrosive and toxic acids, enzymatic hydrolysis processes with long duration, or multiple processing steps. For instance, processes including two stages of enzymatic hydrolysis[20] or two stages of acid hydrolysis[21] have been reported for mannose production from coffee extraction residues. For açaí seeds, a sequential process of dilute-sulfuric acid and enzymatic hydrolysis was developed to obtain mannose in over 95% yield.[13] This two-step process was necessary because a single step of sulfuric acid hydrolysis was inefficient at releasing mannose, leaving ~70% mannan in the seed, while a single step of enzymatic hydrolysis achieved only 3% mannose yield,[13] demonstrating the polysaccharide's high recalcitrance.

However, since sulfuric acid is toxic and corrosive, it is desirable from both safety and environmental perspectives to develop an alternative process that utilizes a less harmful acid. In addition, limited knowledge of more specific mannanases – required for efficient enzymatic depolymerization of crystalline mannan – further emphasizes the need for greater yields in acid hydrolysis. In this regard, dicarboxylic acids offer a greener and more efficient alternative to sulfuric acid since they are less corrosive, safer to handle and store, and can be produced from renewable resources.[22] In addition, they can efficiently hydrolyze hemicelluloses, particularly xylan, while

limiting the formation of degradation products and achieving higher sugar yields.[22,23] This is possible due to their two pK_a values, which are higher than those of sulfuric acid, resulting in a higher solution pH and enabling an efficient hemicellulose hydrolysis over a range of temperature and pH values.[22–24] Oxalic acid, in particular, is a dicarboxylic acid with strong acidity compared to other organic acids, with pK_a values of 1.27 and 4.28 at 25 °C,[25] which has been shown to be beneficial for xylose production from lignocellulosic biomasses.[23,24,26] Moreover, greener alternatives to the fossil-based production of oxalic acid have been developed, including oxidation of biomass sugars,[27] microbial fermentation,[28,29] and electrochemical routes from CO_2.[30] However, to date, studies investigating biomass hydrolysis with oxalic acid have mainly focused on xylan-rich hemicelluloses,[24,26,31–33] with a few reports on galactomannan hydrolysis[21,34] that had no particular focus on crystalline mannan deconstruction.

Additionally, although the use of organic acids has been demonstrated as efficient for the acid hydrolysis of hemicelluloses, few works have demonstrated the economic viability of biomass fractionation by those processes.[5,35–38] To date, the feasibility of xylo-oligosaccharides,[37] bioethanol,[36] nanocellulose,[35] and an integrated production of xylose, cellulose pulp and lignin[38] have been reported using different organic acids. In a recent study by our group, preliminary evaluation of mannose production was explored through dilute oxalic acid hydrolysis of açaí seeds, under preliminary, non-optimized conditions.

In this work, the operating conditions for açaí seed conversion by hydrolysis using dilute oxalic acid are optimized for mannose production. For this purpose, temperature, time, and acid concentration are optimized through a central composite rotatable design, and the enzymatic digestibility of acid-digested açaí seeds is evaluated in a subsequent enzymatic hydrolysis step, for comparison with a benchmark sulfuric acid–enzymatic hydrolysis process.[13] In addition, techno-economic assessment of a plausible biorefinery processing 47 kt of açaí seeds per year is performed with support from process simulation tools. Thus, this work provides significant advances in mannose production, overcoming challenges that help meeting the principles of green chemistry by using renewable raw materials and less harmful chemicals, improving safety, and reducing waste.

2. Materials and methods

2.1 Materials

Açaí seed samples were kindly provided by the company Açaí Amazonas Ltd (Óbidos, Pará, Brazil) and ground in a knife mill to pass through a 2 mm screen (Universal cutting mill PULVERISETTE 19®, Fritsch, Idar-Oberstein, Germany). The seeds were milled without any prior separation of the external mesocarpic fiber layer, which corresponded to approximately 6% of the whole seed weight.[13] Hence, for the sake of brevity, the term 'açaí seeds' used in this study refers to seeds with the

fibrous mesocarpic layer. Mannanase BGM "Amano" 10 was kindly provided by Amano Enzyme Inc. (Nagoya, Japan). Oxalic acid (98%, Sigma-Aldrich, USA) and all other chemicals were purchased from commercial sources and utilized without additional purification.

2.2 Dilute-oxalic acid hydrolysis

Acid hydrolysis assays were performed with a solid/liquid ratio of 1 : 4 in 120 mL round-bottom pressure tubes (Ace Glass, Vineland, NJ, USA) containing 3–5 g (dry weight) of milled açaí seeds and 12–20 mL of dilute-oxalic acid solution with concentrations ranging from 1.48% to 6.5% (w/w). The tubes were heated in a glycerin bath at temperatures between 116 °C and 178 °C for a reaction time of 15–65 min. The ramping time to reach the reaction temperature ranged from 2 to 7 min, but the ramp-up period was not included when calculating the reaction time, which was assumed to start only when the target temperature was reached.

After hydrolysis, the tubes were cooled in a water bath and 64 mL of deionized water were added to each tube. The tubes' contents were then filtered, and samples of the liquid streams (hydrolysates) were withdrawn and prepared for chromatographic analysis to quantify sugars and degradation products. In addition, a mild post-acid-hydrolysis was performed in triplicate using 5 mL of each hydrolysate in order to hydrolyze and indirectly measure the remaining oligosaccharides. For that, concentrated sulfuric acid was added to the samples to reach a final concentration of 4% (w/w) H_2SO_4 and the post-acid-hydrolysis was carried out at 121 °C for 1 h, as described by Sluiter *et al.*[39] Acid hydrolysis yields of mannose ($Y_{1/0}$) and MOS (Y_{MOS}) were calculated according to eqn (1a) and (1b), respectively.

$$Y_{1/0} = \nu C_1 V_1 / (m_0^{db} w_0^{db}) \tag{1a}$$

$$Y_{MOS} = \nu (C'_1 - C_1) V_1 / (m_0^{db} w_0^{db}) \tag{1b}$$

where $\nu = (180 - 18)/180 = 0.9$ is a constant stoichiometric parameter, defined as the ratio between the molecular weight of mannan and mannose, C_1 is the mannose concentration in the acid hydrolysate (in g L^{-1}), C'_1 is the mannose concentration in the hydrolysate after the mild post-acid hydrolysis with H_2SO_4 (in g L^{-1}), V_1 is the volume of oxalic acid solution in the hydrolysis assay (in L), m_0^{db} is the initial dry-basis mass of açaí seeds in the hydrolysis assay, and w_0^{db} is the initial mannan content of açaí seeds on a dry-weight basis, as determined by compositional analysis assays.

The residual solids recovered after dilute-oxalic acid hydrolysis and filtration (*i.e.*, acid-hydrolyzed açaí seeds) were dried at 40 °C until reaching less than 10% moisture for further characterization and enzymatic hydrolysis assays. Additionally, for each hydrolysis condition, a sacrifice assay was performed for mass loss determination, in which the residual solids were filtered in preweighed fiber glass filters and dried in an oven at 105 °C overnight. The fraction of mass loss in acid hydrolysis with oxalic acid (δ_1) was calculated according to eqn (2).

$$\delta_1 = 1 - m_1^{db} / m_0^{db} \tag{2}$$

where m_1^{db} is the final dry-weight mass of açaí seeds recovered after acid hydrolysis and m_0^{db} is the initial dry-weight mass of açaí seeds in the hydrolysis assay.

2.3 Experimental design and statistical analysis

The effects of temperature, acid concentration, and reaction time were analyzed through a central composite rotatable design. Additionally, these effects were handled as a single parameter, the combined severity factor (CSF),[40] to analyze sugar yields across the different conditions. The CSF is defined in eqn (3) as a function of the pH of the solution, the reaction time (t) in min, and the operating temperature (T) in °C.[40] Table 1 displays the values and levels of the independent variables, as well as the resulting CSF for each condition. In addition, Fig. S1 of the ESI† presents the pH values of oxalic acid solutions used for calculating CSF values.

$$CSF = -pH + \log[t \times \exp((T - 100)/14.75)] \tag{3}$$

The mannose yield, mannan conversion, and fraction of mass loss in acid hydrolysis with oxalic acid ($Y_{1/0}$, χ_1, δ_1) were chosen as response variables. A total of 17 independent experiments were performed, including 3 replicates of the central point. Regression analysis was performed for each response variable and second-order models were obtained and analyzed statistically by analysis of variance (ANOVA) using the statistical software Protimiza experimental design (**https://experimental-design.protimiza.com.br**). Model validation experiments were performed in triplicate and the results were analyzed for differences among means *via* the Tukey test ($p < 0.05$).

Table 1 Experimental conditions and combined severity factor for dilute-oxalic acid hydrolysis of açaí seeds according to the central composite design. Coded values of the variables are indicated in parentheses

Run number	Temperature (x_1, °C)	Acid concentration (x_2, %w/w)	Time (x_3, min)	Combined severity factor
1	130 (−1)	2.5 (−1)	25 (−1)	1.16
2	170 (+1)	2.5 (−1)	25 (−1)	2.33
3	130 (−1)	5.5 (+1)	25 (−1)	1.30
4	170 (+1)	5.5 (+1)	25 (−1)	2.47
5	130 (−1)	2.5 (−1)	55 (+1)	1.50
6	170 (+1)	2.5 (−1)	55 (+1)	2.68
7	130 (−1)	5.5 (+1)	55 (+1)	1.64
8	170 (+1)	5.5 (+1)	55 (+1)	2.82
9	116.4 (−1.68)	4.0 (0)	40 (0)	1.04
10	178.0 (+1.4)[a]	4.0 (0)	40 (0)	2.86
11	150 (0)	1.5 (−1.68)	40 (0)	1.86
12	150 (0)	6.5 (+1.68)	40 (0)	2.12
13	150 (0)	4.0 (0)	14.8 (−1.68)	1.60
14	150 (0)	4.0 (0)	65.2 (+1.68)	2.24
15	150 (0)	4.0 (0)	40 (0)	2.03
16	150 (0)	4.0 (0)	40 (0)	2.03
17	150 (0)	4.0 (0)	40 (0)	2.03

[a] The temperature was kept at 178 °C due to a technical limitation of the glycerin bath.

2.4 Enzymatic hydrolysis

Enzymatic hydrolysis of acid-hydrolyzed açaí seeds was performed in 25 mL flasks with a total assay mass of 10 g using 2% (w/w) solid loading in 0.05 M sodium citrate buffer (pH 4.8). The β-mannanase activity loading was 250 IU g^{-1} dry biomass and the mannanase activity was measured according to a procedure reported by Monteiro *et al.*[13] The flasks were incubated in a shaker at 50 °C and 200 rpm for 72 h, after which time the enzymatic reaction was stopped by heating the samples in a water bath at 100 °C for 5 min. Then, the samples were centrifuged, filtered and frozen until HPLC analysis was performed for sugar quantification. Mannose yields were calculated in relation to the mannan content of acid-hydrolyzed açaí seeds ($Y_{2/1}$), according to eqn (4).

$$Y_{2/1} = \nu C_2 V_2 / (m_2^{db} w_1^{db}) \qquad (4)$$

where ν is a constant stoichiometric parameter equal to 0.9, C_2 is the mannose concentration after 72 h of enzymatic hydrolysis (in g L^{-1}), V_2 is the initial volume of the enzymatic hydrolysis assay (in L), m_2^{db} is the dry-weight mass of acid-hydrolyzed açaí seeds used in the enzymatic hydrolysis assay (in g), and w_1^{db} is the mannan content of acid-hydrolyzed açaí seeds on dry-weight basis.

The mannose yield in the enzymatic hydrolysis was also calculated in relation to the initial mannan content of untreated açaí seeds ($Y_{2/0}$) according to eqn (5), and the total yield of acid and enzymatic hydrolyses in the series ($Y_{mannose}^{total}$) was obtained from eqn (6).

$$Y_{2/0} = Y_{2/1}(1 - \delta_1)w_1^{db}/w_0^{db} \qquad (5)$$

where $Y_{2/1}$ is the mannose yield in the enzymatic hydrolysis in relation to the mannan content of acid-hydrolyzed açaí seeds, δ_1 is the fraction of mass loss in the acid hydrolysis reaction, and w_0^{db} and w_1^{db} are the mannan contents of *in natura* and acid-hydrolyzed açaí seeds, respectively, on a dry-weight basis.

$$Y_{mannose}^{total} = Y_{1/0} + Y_{2/0} \qquad (6)$$

where $Y_{1/0}$ is the mannose yield of the acid hydrolysis (obtained from eqn (1a)) and $Y_{2/0}$ is the mannose yield of the enzymatic hydrolysis on the basis of the mannose potential of *in natura* açaí seeds (obtained from eqn (5)).

2.5 Chemical compositional analysis

Chemical compositional analyses of acid-hydrolyzed and *in natura* açaí seed samples were performed in triplicate using the procedure provided by the National Renewable Energy Laboratory (NREL).[41] Briefly, 0.3 g (dry weight) of biomass samples were subjected to an acid hydrolysis process in two steps: (1) with 3 mL of 72% (w/w) H$_2$SO$_4$ for 1 h at 30 °C; (2) followed by dilution to 4% (w/w) H$_2$SO$_4$ with distilled water and a second hydrolysis process at 120 °C for 1 h. Then, the samples were filtered through preweighed Gooch crucibles and the acidic liquors were analyzed by HPLC for sugar quantification. The remaining solids were dried at 105 °C overnight and subsequently placed in a muffle furnace at 575 °C for at least 4 h to obtain the solids' acid insoluble ash content. The content of acid resistant solids (ARS) in açaí seed samples was calculated from the dry weight of the remaining solids excluding their acid insoluble ash content.

Following the determination of the mannan content in the *in natura* and acid-hydrolyzed açaí seed samples, the fraction of unconverted mannan (u_1) in the residual solids was calculated in relation to the mannose potential of *in natura* açaí seeds, according to eqn (7). Finally, the percentage of mannan conversion (χ_1) was calculated through eqn (8).

$$u_1 = (1 - \delta_1)w_1^{db}/w_0^{db} \qquad (7)$$

$$\chi_1 = 1 - u_1 \qquad (8)$$

2.6 Analytical methods

Concentrations of sugars (mannose, glucose, xylose, and galactose) and degradation products (HMF and furfural) were quantified by HPLC (Ultimate 3000 system, Thermo Scientific, Waltham, MA, USA) equipped with a refraction index detector (RI-101, Shodex, Japan). For sugar quantification, an Aminex HPX-87P column was used (300 × 7.8 mm, Bio-Rad Laboratories, Hercules, CA, USA), with a Carbo-P precolumn and an inline deashing system (both Bio-Rad Laboratories, Hercules, CA, USA). Ultrapure water was used as the mobile phase at a flow rate of 0.6 mL min^{-1} and the oven and detector temperatures were 80 °C and 50 °C, respectively. HMF and furfural were quantified using an Aminex HPX-87H column (300 × 7.8 mm, Bio-Rad Laboratories, Hercules, CA, USA) with a Carbo-H precolumn and an inline deashing system (both Bio-Rad Laboratories, Hercules, CA, USA). The mobile phase was 5 mM H$_2$SO$_4$ at a flow rate of 0.6 mL min^{-1}, the oven temperature was 55 °C, and the detector temperature was 50 °C. Concentrations were calculated using external calibration curves obtained from standard solutions.

2.7 Techno-economic analysis

The economic viability of commercial-scale mannose and MOS production by dilute oxalic acid hydrolysis was evaluated based on process simulations. The techno-economic analysis assumed a processing capacity of 6000 kg h^{-1} (dry basis) of açaí seeds in continuous mode and the process design was based on a previous study by our group,[5] which evaluated mannose production from açaí seeds *via* oxalic acid hydrolysis using preliminary, non-optimized data. Here, an updated economic evaluation is presented with two main modifications: recovery of MOS syrup as a coproduct, along with recovery and recycling of oxalic acid, thus minimizing acid purchase, while eliminating the need for hydrolysate neutralization and avoiding salt waste generation. Experimental data from oxalic acid hydrolysis and subsequent enzymatic hydrolysis were used to simulate mannan depolymerization, while purification processes for oxalic acid, mannose, and MOS were based on literature data for related processes. Fig. 1 shows a block flow diagram of the simulated biorefineries, while oper-
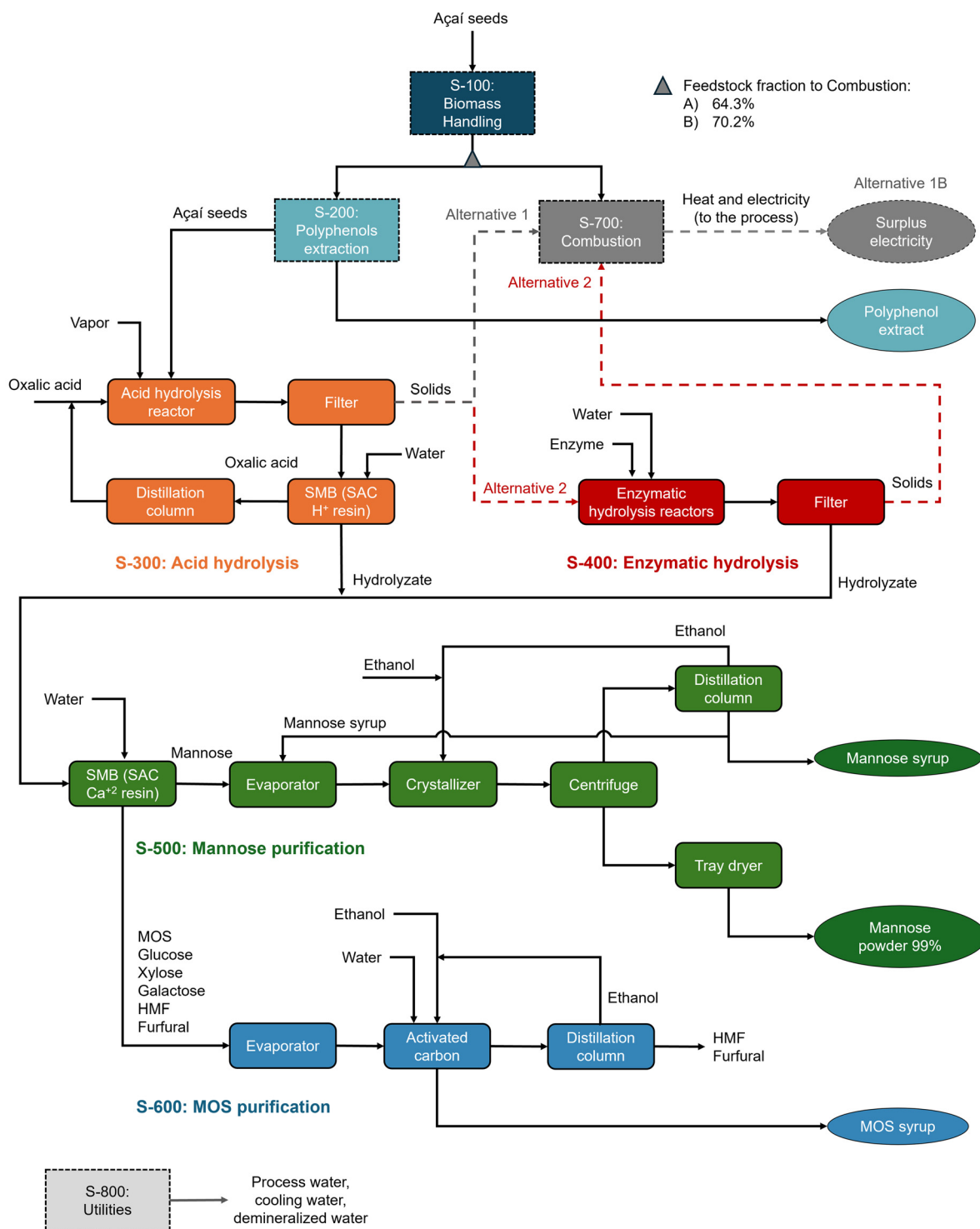
Fig. 1 Block flow diagram of biorefinery alternatives for processing açaí seeds into mannose in powder and syrup form, MOS syrup, and polyphenol extract. SMB: simulated moving bed chromatography; SAC: strong acid cation exchange resin.

ating parameters considered in the process simulations are detailed in the ESI.†

2.7.1 Process simulation. Process simulations were performed in Aspen Plus® V8.8 (AspenTech) using the nonrandom two liquid (NRTL) and Redlich-Kwong equation-of-state (RK-EOS) thermodynamic models for the liquid and vapor phases, respectively, except for acid hydrolysis and acid recovery equipment, where the Aspen Plus Electrolyte NRTL model coupled to RK-EOS was employed. The açaí seed chemical composition was calculated as a normalized average of

experimental results from this study and two works reported in the literature,[13,14] which can be found in the ESI.† The thermodynamic parameters and physicochemical properties of biomass components were retrieved from the literature.[42]

The simulated process was divided into eight process sections (Fig. 1). Initially, açaí seeds are pre-conditioned in section S-100, which includes washing, drying, and milling operations, and are subsequently extracted with 50%w aqueous ethanol in section S-200, generating a polyphenolic extract as a coproduct.[5] In section S-300, açaí seeds undergo oxalic acid hydrolysis in a continuous screw reactor and oxalic acid recovery is performed through continuous simulated moving bed (SMB) ion-exclusion chromatography. In this process, ionic species, such as dissociated acids, are eluted first due to ion exclusion from a strong acid cation (SAC) resin, while sugars are adsorbed on the resin and further eluted with water.[43,44] The oxalic acid stream leaving the SMB is concentrated to 40%w in a distillation column and recycled to the acid hydrolysis reactor, while the distillate (water) is recycled by SMB chromatography. When sequential enzymatic hydrolysis is considered, the solids exiting S-300 are sent to batch reactors in S-400 that operate at 20% solid loading and with 250 IU mannanase per g biomass. The residual solids from enzymatic hydrolysis are sent for combustion (S-600), while the hydrolysate is mixed with the acid hydrolysate for further processing.

For mannose separation from other sugars and impurities (S-500), another SMB with a strong acid cation resin is used, preferably in Ca^{2+} form.[45–47] The highly pure mannose stream is concentrated to 70%w in a multi-effect evaporator system and crystallized with ethanol to produce 99%w powdered mannose. The mother liquor leaving the crystallizer is sent to a distillation column, from which ethanol (distillate) is recycled back to the crystallizer and mannose syrup (bottom) is partly (50%) recycled to the evaporator and partly sold as a coproduct with 55°Brix (55 g sugars per 100 g solution). On the other hand, the MOS-rich raffinate stream from the SMB is concentrated and sent for activated carbon treatment to remove HMF and furfural[48,49] (S-600), producing a MOS-rich sugar syrup with 55°Brix for commercialization. The impurities are desorbed from activated carbon with 90% ethanol, which is further distilled and recycled in the process.

2.7.2 Economic evaluation. The mass and energy balances obtained from process simulations were used for estimating equipment sizes and process demands of raw materials and utilities, which were the basis for economic analysis. Equipment costs were calculated with the CAPCOST spreadsheet using the methods of Turton *et al.*,[50] which were also employed for estimating the fixed capital investment (FCI) and cost of manufacturing (COM). This type of early-stage FCI estimation, based on equipment cost models established in the literature, is classified as a Class 4 cost estimate by the AACE (Association for the Advancement of Cost Engineering), with a typical accuracy range of −30% to +50%.[51,52] Finally, cash flow analysis was performed to calculate the project's financial indi-

Table 2 Economic premises for the techno-economic analysis[a]

Item	Value	Unit
CEPCI	816	
Taxation rate	34	%
Annual interest rate	10	%
Depreciation rate	10	%
Working capital	15	%FCI[b]
Plant availability	7880	h per year
Project lifetime	20	Years
Construction period	3	Years
FCI expenditure in the 1st, 2nd, and 3rd years of construction	40/30/30	%FCI
Operator labor cost[53]	14 352	US$ per year
Product selling prices		
Mannose[5]	10.00	US$ per kg
Polyphenolic extract[5]	5.00	US$ per kg
Mannose syrup[54]	2.00	US$ per kg (dry weight)
MOS syrup[c]	2.00	US$ per kg (dry weight)
Electricity[55]	121.46	US$ per MWh
Costs of raw materials and utilities		
Açaí seeds[5]	27.22	US$ per t
Ethanol[5]	0.694	US$ per kg
Oxalic acid[5]	0.833	US$ per kg
Enzyme[5]	21.50	US$ per kg
Activated carbon[56]	6.00	US$ per kg
Chromatography resins[5]	2.27	US$ per m³ feed
Process water[5]	0.28	US$ per m³

[a] For references with prices in Brazilian currency (R$), the exchange rate was standardized as US$ 1.00 being equal to R$ 5.00. [b] FCI: fixed capital investment. [c] Based on the prices of fructooligosaccharide and isomaltooligosaccharide syrups.[57,58]

cators, namely, the net present value (NPV), the internal rate of return (IRR), and the discounted payback period. Detailed economic premises, parameters and prices are summarized in Table 2.

3. Results and discussion

3.1 Optimization of dilute-oxalic acid hydrolysis of açaí seeds

The hydrolysis of açaí seeds was performed with dilute-oxalic acid solutions in order to depolymerize its high mannan content and optimize mannose production. The mannan content of *in natura* açaí seeds used in this study was 50.6% ± 0.6%, which was in agreement with previously reported compositions of açaí seeds that ranged from 47.0% to 52.5% of the seeds' total dry weight.[13,14] Other components of açaí seeds included: 5.8% ± 0.9% glucan, 1.8% ± 0.2% xylan, 1.3% ± 0.2% galactan, 11.8% ± 0.3% extractives, 20.8% ± 1.2% acid resistant solids (ARS), and 1.6% ± 0.1% ash. ARS corresponded to the organic matter that was resistant to concentrated sulfuric acid hydrolysis (as described in section 2.5) and did not include acid insoluble ash.

After performing the acid hydrolysis assays according to the central composite rotatable design (as outlined in Table 1), the hydrolysates and residual solids were analyzed to determine the response variables. The results are summarized in Table 3, including the mannose concentration and yield of the hydroly-

Table 3 Mass loss, mannose concentration and yield, mannan conversion, and residual solid composition following dilute-oxalic acid hydrolysis of açaí seeds

Run	CSF[a]	Mass loss (%)	Hydrolysate mannose concentration[b] (g L^{-1})	Mannose yield[c] (%)	Residual solid composition (% dry weight)[d]			Mannan conversion[f] (%)
					Mannan	Glucan	ARS[e]	
1	1.16	19.5	7.7 [17.4]	5.5	52.0 ± 1.0	8.8 ± 0.7	28.1 ± 1.9	17.2
2	2.33	59.7	97.9 [113.0]	69.7	26.6 ± 2.2	17.5 ± 3.8	50.0 ± 2.2	78.8
3	1.30	25.6	18.5 [20.9]	13.2	50.4 ± 1.8	7.8 ± 1.5	26.6 ± 0.8	25.8
4	2.47	71.9	113.1 [128.7]	80.5	6.7 ± 2.8	19.3 ± 1.2	64.2 ± 1.9	96.3
5	1.50	27.1	23.5 [25.5]	16.7	53.4 ± 1.0	7.6 ± 1.5	32.3 ± 1.7	23.1
6	2.68	70.9	107.4 [119.3]	76.5	11.5 ± 2.9	16.4 ± 1.8	61.5 ± 3.0	93.4
7	1.64	34.7	47.4 [48.0]	33.8	47.7 ± 3.0	8.2 ± 1.4	31.4 ± 2.6	38.4
8	2.82	71.6	89.6 [96.0]	63.8	0.7 ± 0.4	18.5 ± 0.4	68.4 ± 2.1	99.6
9	1.04	18.2	11.6 [23.5]	8.3	49.0 ± 0.7	7.5 ± 0.2	35.3 ± 2.0	20.8
10	2.86	72.3	91.2 [98.2]	64.9	3.0 ± 0.0	24.2 ± 0.4	69.8 ± 2.1	98.3
11	1.86	31.1	49.6 [51.1]	35.3	51.0 ± 0.7	10.2 ± 0.8	33.0 ± 1.0	30.5
12	2.12	50.2	85.7 [91.8]	61.0	34.7 ± 2.6	17.5 ± 1.2	46.0 ± 2.2	65.8
13	1.60	35.0	52.2 [56.3]	37.2	47.1 ± 0.5	9.8 ± 0.5	37.0 ± 2.2	39.4
14	2.24	47.9	81.2 [87.5]	57.8	42.7 ± 1.2	12.7 ± 0.3	40.2 ± 1.0	55.9
15	2.03	46.6	75.9 [87.9]	54.1	38.5 ± 1.3	10.3 ± 2.3	39.0 ± 2.3	59.3
16	2.03	44.8	76.5 [86.7]	54.5	40.2 ± 1.9	11.2 ± 2.1	41.4 ± 3.4	56.1
17	2.03	43.6	73.2 [85.3]	52.1	42.0 ± 1.6	8.1 ± 4.2	40.7 ± 2.7	53.1

[a] Combined severity factor. [b] Values in brackets correspond to the mannose concentration in the hydrolysates after a mild post-acid hydrolysis (4% H_2SO_4, 121 °C, 1 h), which releases mannose from the hydrolysates' mannanoligosaccharides (MOS). [c] Refers only to mannose, excluding the MOS content of the hydrolysates. [d] The contents of xylan and galactan detected in the residual solids were below 2% of the sample dry weights and are not shown. [e] Acid resistant solid. [f] Mannan conversion is expressed as a percentage of the total mannan content of *in natura* seeds.

sates, mass loss, the chemical composition of recovered unhydrolyzed residual solids, and mannan conversion.

Mannose was the main sugar detected in the hydrolysates, with concentrations ranging from 7.7 g L^{-1} under the lower severity conditions up to 113.1 g L^{-1} at a CSF of 2.47 (Table 3), while glucose was the second major monosaccharide with concentrations between 0.5 and 6.6 g L^{-1}. Xylose and galactose were detected in smaller amounts (2.2 and 2.6 g L^{-1} on average, respectively), which was consistent with the low content of these sugars in the *in natura* seed.

A broad range of results was observed for all responses: 5.5–80.5% mannose yield, 19.5–72.3% mass loss, and 17.2–99.6% mannan conversion, evincing that the chosen conditions for the experimental design were sufficient to describe the reaction space (Table 3). Interestingly, strong correlations were observed between the CSF and the response variables (Fig. S2 in the ESI†). A CSF range of 2.3 to 2.7 resulted in high mannose yields of 70–80%, with accordingly high values of mannan conversion (79–96%) and mass loss (60–72%). The maximum mannose concentration (113.1 g L^{-1}) and yield (80.5%) were attained with 5.5% (w/w) oxalic acid at 170 °C for 25 min, corresponding to a CSF of 2.47 (run 4, Table 3). Above this severity level, mannose yields decreased while mannan was completely hydrolyzed. For instance, 63.8% of mannose yield was attained with 99.6% of mannan conversion at CSF 2.82 (run 8, Table 3), indicating the occurrence of undesired mannose degradation reactions.

To the best of our knowledge, this is the first report of an organic acid-catalyzed depolymerization of crystalline mannan with mannose yields as high as 80% in only one step. The use

of oxalic acid for açaí seed hydrolysis has been reported at 3.0% (w/w), 121 °C for 60 min but these conditions resulted in only 16.54% of mannan solubilization, while using sulfuric acid under the same conditions led to 28.7% yield, thus requiring a second enzymatic hydrolysis step for complete mannan depolymerization.[59] To date, few studies have investigated the use of acid hydrolysis for the depolymerization of mannan from açaí seeds. For example, when employing sulfuric acid for açaí seed hydrolysis, Monteiro *et al.* reported a maximum mannose concentration and yield of 49.5 g L^{-1} and 34%, respectively, which was achieved with 4.5% (w/w) sulfuric acid at 121 °C for 60 min, equivalent to a CSF of 1.7.[13] Our results show that at a similar CSF of 1.64 (130 °C, 5.5% w/w, 55 min), oxalic acid-catalyzed hydrolysis leads to an analogous mannose concentration and yield of 47.4 g L^{-1} and 33.8%, respectively (run 7, Table 3).

Another study reported optimal hydrolysis conditions for açaí seeds employing 3.5% (w/v) H_2SO_4 at 121 °C for 70 min with 25% (w/v) of solids, which resulted in a comparable mannose concentration of 51 g L^{-1}.[60] The authors also reported a maximum concentration of total reducing sugars of 103 g L^{-1} at 4% (w/v) H_2SO_4, 20% (w/v) of solids, and 121 °C for 90 min (CSF 1.68).[60] Although the mannose yield was not reported, it could be roughly estimated as between 78% and 85% based on the typical mannan content of açaí seeds (50–55%).[13,14] Nevertheless, these conditions resulted in the formation of 0.45 g L^{-1} of HMF, and thus was not considered as optimal in the study.[60] Our results evince that oxalic acid hydrolysis enables a comparable mannose yield of 80.5% (run 4, Table 3) at a higher CSF of 2.47 while producing 3.2 g L^{-1} of

HMF, whereas hydrolysis at a similar CSF of 1.64 leads to a lower mannose yield (33.8%) and negligible HMF formation (0.09 g L^{-1}). Nevertheless, the comparison of HMF levels is limited by differences in hydrolysis conditions in both studies, namely, temperature and time, which directly influence the activation energy for sugar degradation and the extent of degradation depends on the type of acid – mineral or dicarboxylic.[61] Moreover, despite the higher concentration of HMF, hydrolysis by oxalic acid offers important advantages for commercial operation regarding safety and environmental aspects due to its lower toxicity compared to sulfuric acid.[22]

Here, HMF levels were not considered as a selection criterion because the açaí seed hydrolysate was not intended to be used in a subsequent enzymatic hydrolysis or fermentation process. In addition, purification strategies can be applied to remove HMF and other degradation compounds from the final product, while mannose concentration and yield are more important drivers for economic viability.[5] Therefore, mannose yield was the main criterion for process optimization in this work.

Other work has described the use of oxalic acid for mannose production from galactomannan-rich coffee bean extraction residues; however, organic acid hydrolysis was followed by a second hydrolysis step using a solid acid in order to achieve yields of ~80%.[21] The need for a multi-step hydrolysis process to obtain mannose and MOS is directly dependent on the mannan polysaccharide's structure and recalcitrance. Water soluble mannans (α-mannans, gluco-, galacto-, and glucogalactomannans) can be extracted under mild conditions[62–65] or depolymerized in over 80% yield in a single-step acid,[66,67] enzymatic[68,69] or hydrothermal hydrolysis process.[70] On the other hand, more recalcitrant mannans, such as linear mannans from palm seeds and less branched galactomannans from coffee beans, typically require multi-step processes involving sequential pretreatments and enzy-

matic hydrolysis to obtain mannose and MOS in over 80% yield.[13,20,71,72] Nevertheless, our results demonstrate that the combination of factors (temperature, time, and acid concentration) in acid hydrolysis can enable the efficient depolymerization of linear mannan, achieving high mannose yields in a single-step process, without a subsequent enzymatic hydrolysis step.

In addition to mannose, the oxalic acid hydrolysis of açaí seeds leads to the coproduction of MOS with concentrations ranging from 0.5 to 15.6 g L^{-1} (Table 3), indirectly quantified by a mild post-acid hydrolysis step with sulfuric acid. The conditions with the highest mannose yield (170 °C, 5.5%, 25 min) also displayed the highest MOS production, with 11.1% MOS yield and a combined yield of 91.6% considering both products of interest. While the production of MOS from açaí seeds has been reported via enzymatic hydrolysis, achieving 12 g L^{-1} under optimized conditions,[73] there are no studies on their production through dicarboxylic acid hydrolysis. Nevertheless, the coproduction of mono- and oligosaccharides is in accordance with other studies that demonstrate that organic acids are more beneficial for the production of xylooligosaccharides than conventional sulfuric acid.[37,74,75]

The mannose mass balances in both liquid and solid fractions after oxalic acid hydrolysis are shown in Fig. 2, where the hydrolysis conditions are displayed in ascending order of CSF. Overall, an increase in CSF up to 2.09 results in a tendency of higher mannose yield in the hydrolysate ($Y_{1/0}$) and less unconverted mannan in the residual solids (u_1), with mass balance closures over 95%. For higher severities, the mannan content in the solid fraction is drastically reduced and the low mass balance closures indicate that mannose is converted into degradation products. Indeed, HMF levels reached 9.0 g L^{-1} under the highest severity conditions (run 10, CSF 2.86), while at CSF 2.09 (run 2) and CSF 2.38 (run 4) HMF concentrations were 1.2 g L^{-1} and 3.2 g L^{-1}, respectively.
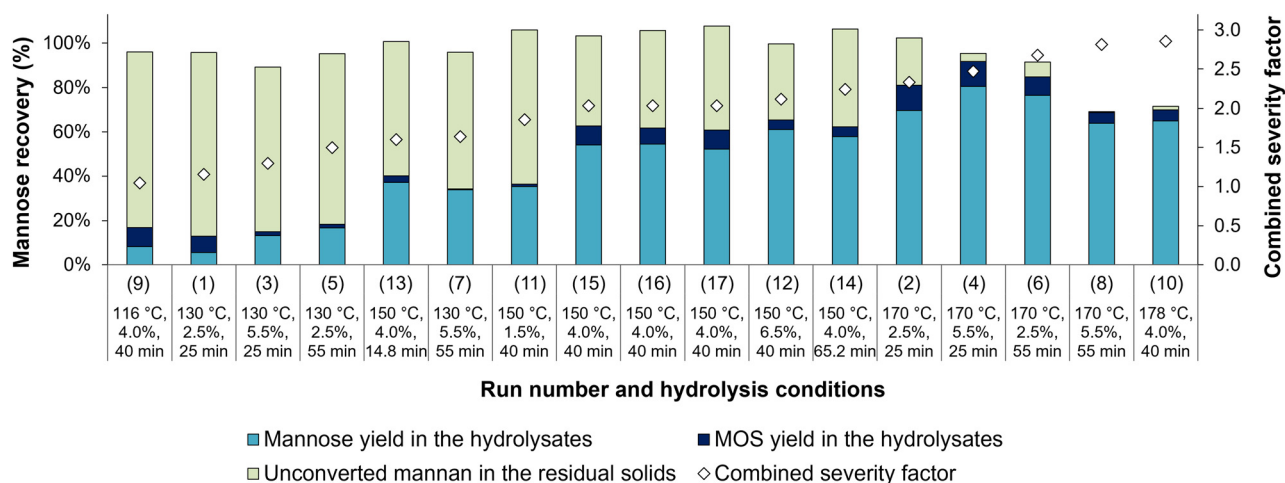
Fig. 2 Mannose mass balances in the hydrolysates and residual solids after dilute-oxalic acid hydrolysis of açaí seeds. Mannose recoveries include mannose and MOS yields in the hydrolysates and unconverted mannan in the residual solids, all expressed as a percentage of the total mannose potential of *in natura* seeds.

Several studies have demonstrated how dicarboxylic acids can hydrolyze hemicellulose as effectively as sulfuric acid while limiting sugar degradation side reactions. Early work by Lu and Mosier[61] hypothesized that such selectivity of dicarboxylic acids towards the hydrolysis of β-(1,4)-bonds could arise from a "biomimetic" cooperative mechanism between their two carboxylate groups in close proximity, which would mimic the active site of glycosidases.[61] Nevertheless, enzyme computational studies revealed that the cooperative mechanism between carboxylic acid moieties in glycosidase amino acid residues relied on specific microenvironment conditions of the enzyme's active site, where the dielectric constant and electrostatic potential built by the protein did not reflect the conditions of the bulk reaction medium.[25] In addition, experimental results have shown that glucose yields from cellobiose acid hydrolysis depend exclusively on the acidity of the reaction media, regardless of the nature of the acid – mineral, mono- or dicarboxylic – and that HMF formation is negligible at short reaction times.[25] Kusema et al. reported similar findings for the hydrolysis of O-acetyl-galactoglucomannan, where the hydrolysis rate was exclusively dependent on the solution pH and indifferent to the type of acid, while no side products were observed at 90 °C in the pH range of 0.5–2.0.[66]

When a broad range of conditions are evaluated and sugar degradation becomes relevant, mechanistic and kinetic models are useful to analyze hemicellulose hydrolysis while considering an intricate set of reactions leading to the formation of HMF, furfural and other by-products.[76,77] Degradation of xylose has long been investigated with such models, demonstrating that organic acids have a significantly lower activation energy for hydrolysis than for degradation, as opposed to sulfuric acid, which displays an activation energy for xylan hydrolysis strictly higher than that for xylose degradation.[76] Advantages of organic acids over sulfuric acid were also reported in a study on the kinetics of arabinose degradation, also showing that arabinose degraded less readily than xylose and glucose, demonstrating the importance of the careful selection of an acid targeted to a specific polysaccharide depolymerization process.[78]

In this context, the use of oxalic acid for linear mannan hydrolysis, as explored in the present work, showed relevant advantages over sulfuric acid, resulting in 80% mannose yield and enabling the simultaneous production of MOS without significant progression to degradation products, which was not expected for sulfuric acid hydrolysis processes according to the proposed mechanistic models.

3.2 Statistical models

From the experimental data, a regression analysis was performed to build second order models for each response; these are detailed in the ESI.† The analyses of variance (ANOVA) of the fitted models revealed that they were significant with a p-value of <0.0001. The models showed excellent correlation with the data, with R^2 of 90.22% for mannose yield ($Y_{1/0}$), 97.13% for mannan conversion (χ_1), and 97.58% for mass loss (δ_1) in acid hydrolysis (Table S9 in the ESI†).

Fig. 3 displays two-dimensional contour plots of the fitted models for mannose yield ($\hat{Y}_{1/0}$), mannan conversion ($\hat{\chi}_1$), and mass loss ($\hat{\delta}_1$) in acid hydrolysis. For mannose yield, strong interactions between temperature ($x_1 = T$) and the other two factors are observed at high temperature levels, but with opposite effects resulting from an increase in the hydrolysis duration ($x_3 = t$) or acid content in the solution (x_2). Hence, high mannose yields are favored with high temperature and high acid concentration but with reduced time (Fig. 3a). In contrast, mass loss and mannan conversion at high temperatures show an increase when the levels of both time and acid concentration are higher (Fig. 3b and c). This suggests that mannose conversion into degradation products is especially intensified by a combination of high temperature and long hydrolysis duration, reflecting the lag time between mannan hydrolysis and mannose degradation reactions. This observation is in accordance with kinetic models reported for xylan hydrolysis, which describe furfural formation and reduction of xylose yields at prolonged hydrolysis times, with greater effects being observed as the reaction temperature increases.[79] Other work reported similar findings for xylan hydrolysis, where more furfural formation was observed at high treatment temperatures and its appearance was sensitive to both reaction temperature and duration.[80] Thus, the models developed herein for acid hydrolysis bring insights into the kinetic aspects of these reactions, but further studies on the kinetics of mannan hydrolysis are needed to elucidate mannose degradation processes.

3.3 Process validation

Additional hydrolysis experiments were performed in triplicate to validate the second order models obtained for mannose yield and mass loss. Two validation conditions were selected: V1 is the same as the factorial point with the highest mannose yield (170 °C, 5.5% w/w, 25 min); and V2 has the same CSF as V1 but with a shorter duration, thus the temperature and acid concentration are higher (177 °C, 6.0% w/w, 15 min). The predicted values for mannose yield and mass loss under both conditions fit well with the experimental values, with errors below 8%; this demonstrates the accuracy and validity of the models (Table 4).

A comparison of both experiments also shows that the CSF is a useful indicator for selecting hydrolysis conditions since rather similar mannose yields were obtained under the selected conditions with equal severity. Nevertheless, the second order model enables a refined selection of all parameters and predicts a higher yield for validation condition V2 (87.3%) in comparison with V1 (77.2%) (Table 4). Although the predicted values of mannose yield and mass loss under condition V2 were slightly overestimated by the models, the observed values under conditions V1 (76.8% ± 4.5%) and V2 (82.6% ± 3.6%) showed statistically significant differences at a 95% confidence level. Similar to condition V1, MOS were also coproduced under condition V2, reaching a concentration of 13.5 ± 0.4 g L^{-1} and 9.6% ± 0.3% yield in relation to the mannose potential of in natura açaí seeds.
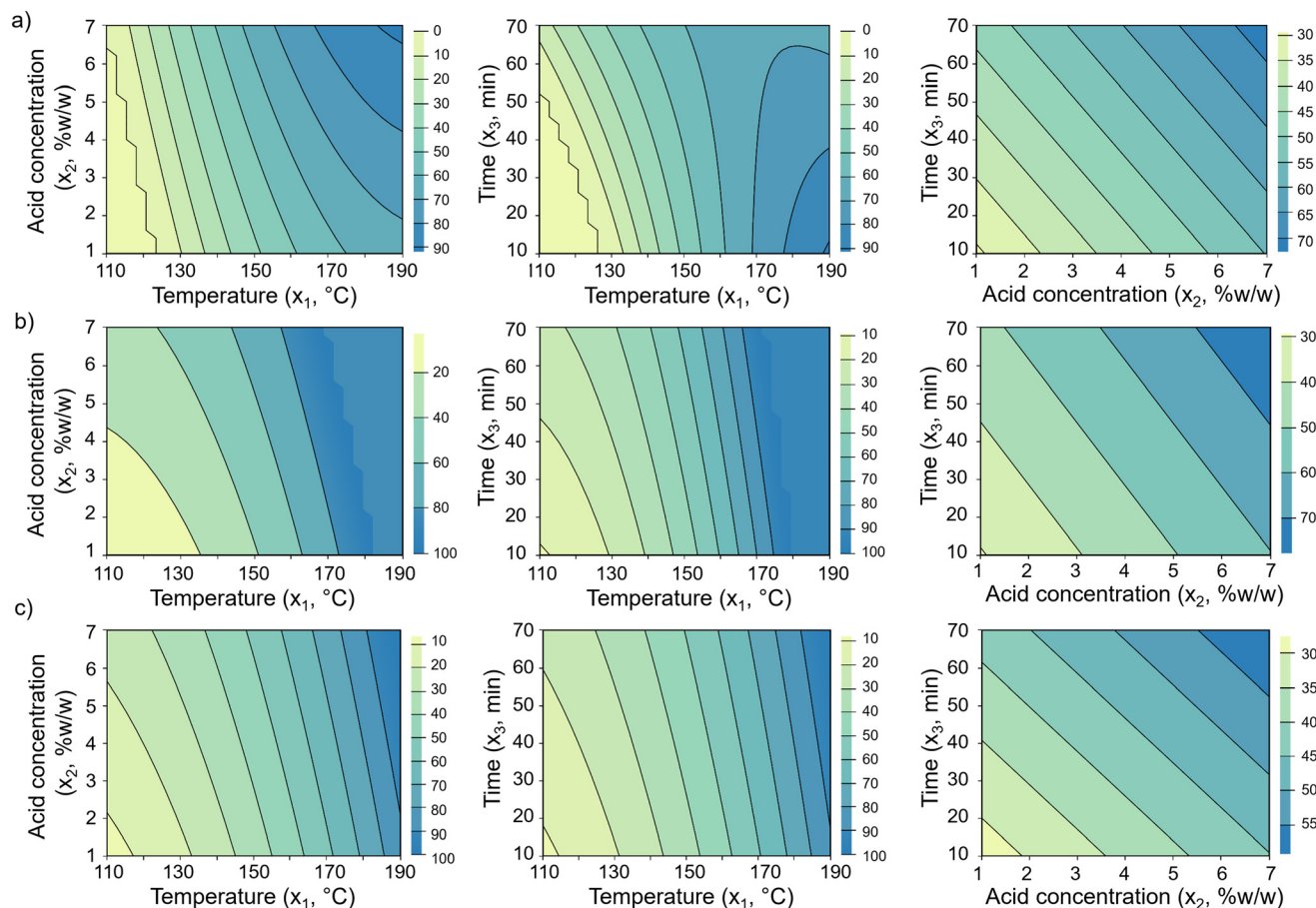
Fig. 3 Contour plots of (a) mannose yield ($\hat{Y}_{1/0}$); (b) mannan conversion ($\hat{\chi}_1$); and (c) mass loss ($\hat{\delta}_1$) obtained from the central composite design for the optimization of açaí seed hydrolysis with dilute oxalic acid. Left column, temperature (x_1, °C) and acid concentration (x_2, %w/w); middle, temperature (x_1, °C) and time (x_3, min); right, acid concentration (x_2, %w/w) and time (x_3, min).

Table 4 Predicted and observed values for mannose yield and mass loss of model validation conditions

Validation condition	Temperature (°C)	Acid concentration (% w/w)	Time (min)	Mannose yield (%)			Mass loss (%)		
				Predicted	Observed	Model error	Predicted	Observed	Model error
V1	170	5.5	25	77.2%	76.8% ± 4.5%	1%	67.1%	67.8% ± 3.2%	−1%
V2	177	6.0	15	87.3%	82.6% ± 3.6%	6%	75.6%	70.6% ± 4.0%	7%

3.4 Enzymatic hydrolysis and total mannose yield

Following acid hydrolysis, solid residues were subjected to enzymatic hydrolysis to determine their digestibility and evaluate whether mannose production could be increased from oxalic acid-hydrolyzed açaí seeds. The solid samples from treatments 8 and 10 were excluded from this analysis since their mannan content was lower than 5%, as determined by compositional analysis (Table 3). Fig. 4 shows the mannose yields in acid hydrolysis (step 1, $Y_{1/0}$ as defined in eqn (1a)) and enzymatic hydrolysis (step 2, $Y_{2/0}$ as defined in eqn (5)) in relation to the mannan content of *in natura* açaí seeds (initial content, subscript 0), which, when summed up, correspond to the total mannose yield of sequential acid and enzymatic hydrolysis ($Y_{\text{mannose}}^{\text{total}}$ as defined in eqn (6)).

In contrast with the trend observed for acid hydrolysis yields, mannose yields from enzymatic hydrolysis did not show a clear increasing tendency with a rise in CSF. Samples treated at temperatures below 150 °C showed limited enzymatic digestibility, with yields below 35% in relation to the mannan content of *in natura* açaí seeds ($Y_{2/0}$) (Fig. 4), and below 45% in relation to the mannan content of acid-hydrolyzed açaí seeds ($Y_{2/1}$ as defined in eqn (4)). This result indicates that oxalic acid treatments at low temperatures (lower than or equal to 130 °C) are inefficient at disrupting the recalcitrant and crystalline mannan structure and increasing its accessibility to enzymes, which is opposite to the high efficiency of sulfuric acid treatments at 120 °C and CSF of 1.4–1.7 that result in enzymatic hydrolysis yields over 95%.[13] Our observations are
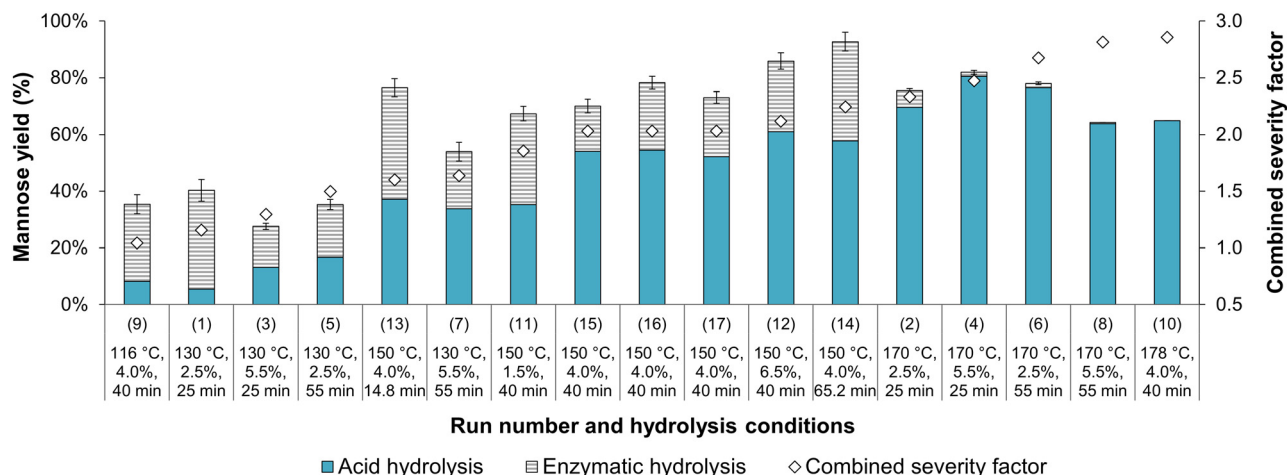
Fig. 4 Mannose yield in the dilute oxalic acid hydrolysis and subsequent enzymatic hydrolysis of açaí seeds, expressed as a percentage of the total mannose potential of *in natura* seeds ($Y_{1/0}$ in blue, $Y_{2/0}$ in dashed gray).

also in contrast to other reports of similar or improved yields in enzymatic hydrolysis of oxalic acid-treated lignocellulosic biomasses in comparison with sulfuric acid under the same hydrolysis conditions.[24,31] Therefore, further investigation is needed to elucidate the structural modifications to açaí seeds' linear mannan after oxalic and sulfuric acid hydrolyses.

For samples treated with oxalic acid at 150 °C, the enzymatic digestibility varied according to the treatment duration and acid concentration. The central point experiments (150 °C, 4.0%, 40 min) displayed low digestibility, with a mannose yield ($Y_{2/0}$) of 20% ± 4% in the enzymatic hydrolysis step and 74% ± 4% total mannose yield ($Y_{mannose}^{total}$) in relation to the seeds' *in natura* mannan content (Fig. 4). Nevertheless, açaí seeds previously treated for a longer time or with higher oxalic acid concentrations resulted in higher enzymatic digestibility. Namely, samples treated with 4.0% w/w oxalic acid at 150 °C for 65.2 min (run 14, CSF of 2.24) showed maximum enzymatic digestibility with a mannose yield of 79% ± 3% in relation to the mannan content of acid-hydrolyzed açaí seeds ($Y_{2/1}$), which corresponded to a mannose yield of 34.9% in relation to the seeds' initial mannan content ($Y_{2/0}$). Combined with an acid hydrolysis yield ($Y_{1/0}$) of 57.8% (Table 3), these conditions achieved a total mannose yield of 92.7% (Fig. 4). A similar result was observed for run 12 with a higher oxalic acid concentration (6.52% w/w) at 150 °C for 40 min (CSF of 2.12), which resulted in a total mannose yield of 85.9%. However, a further increase in CSF and temperature drastically reduced enzymatic hydrolysis yields (runs 2, 4, and 6), suggesting that high severity treatments might disrupt the mannan chains in an inaccessible structure to mannanases. Additional investigation of dilute oxalic acid hydrolysis at temperatures of 150–160 °C is recommended as it may provide optimized total mannose yields and potentially 100% mannan conversion after enzymatic hydrolysis.

3.5 Techno-economic assessment

3.5.1 Process design and simulation. Process simulations were performed to evaluate the economic viability of produ-

cing mannose and MOS by dilute oxalic acid hydrolysis at an industrial scale. In a recent study by our group, an açaí seed biorefinery process employing oxalic acid for mannose production was evaluated technically and economically; this was found to provide significant advantages over a two-step sulfuric acid–enzymatic hydrolysis process even under preliminary non-optimized conditions with a mannose yield of 77.6%.[5] In this work, an updated economic analysis is performed using optimal hydrolysis conditions and including the coproduction of MOS. In addition, oxalic acid recovery and recycling are evaluated, and an additional scenario of sequential oxalic acid hydrolysis and enzymatic hydrolysis is assessed.

Hence, two biorefinery alternatives are compared: alternative 1 considers the one-step acid hydrolysis conditions with the highest mannose yield of 82.6% ($Y_{1/0}$), which employs 6.0% w/w oxalic acid at 177 °C for 15 min (validation condition V2, CSF of 2.47); and alternative 2 considers a sequential process of dilute oxalic acid hydrolysis followed by enzymatic hydrolysis, employing the acid hydrolysis conditions that lead to the highest enzymatic digestibility (4.0% w/w oxalic acid at 150 °C for 65.2 min) and result in the highest total mannose yield of 92.7% ($Y_{mannose}^{total}$). As açaí seeds contain high amounts of polymeric procyanidins,[11,12,81] in both simulations, prior to acid hydrolysis, açaí seeds are extracted with 50%w aqueous ethanol as previously described,[5] producing an antioxidant polyphenol extract as a coproduct and facilitating the later mannose purification steps.

In both alternatives, a processing capacity of 6000 kg h^{-1} (dry basis) of açaí seeds is considered for comparison with our previous study.[5] The biomass feed is partly used for on-site combined heat and power generation *via* combustion, which is presumed because an external power supply in the Brazilian Amazon region would more likely rely on an isolated electrical system based on diesel fuel.[82] In this sense, açaí seeds offer a more sustainable alternative for meeting the process energy demands.[82,83] Initially, the feedstock fraction sent to the combustion section was determined *via* simulation as the

Table 5 Simulation results for process alternatives: açaí seed feed distribution and final product flows. Values in brackets correspond to the mannose yield in relation to the theoretical mannose potential of the mannan feed to biochemical processing. °Bx: Brix (g sugar per 100 g solution)

| Variable	Alternative 1	Alternative 1B	Alternative 2
Split fraction to combustion	64.3%	70.2%	70.2%
Açaí seed feed to combustion (kg h^{-1})	3858	4212	4212
Açaí seed feed to biochemical processing (kg h^{-1})	2142	1788	1788
Mannan feed to biochemical processing (kg h^{-1})	1156	965	965
Product flows			
Mannose powder 99%w (kg h^{-1})	686 [53%]	573 [53%]	614 [57%]
Mannose syrup 55°Bx^a (kg h^{-1})	586 [23%]	490 [23%]	505 [24%]
MOS syrup 55°Bx^b (kg h^{-1})	482 [8%]	403 [8%]	320 [4%]
Polyphenolic extract (kg h^{-1})	233	195	195
Electricity (MW)	—	1.61	—

^{a} Mannose syrup composition: 45% water, 52% mannose, 3% other sugars. ^{b} MOS syrup composition in alternatives 1 and 1B: 43% water, 11% mannose, 21% MOS, 12% glucose, 6% galactose, 6% xylose; and alternative 2: 44% water, 14% mannose, 13% MOS, 13% glucose, 9% galactose, 6% xylose.

minimum amount required to achieve energy self-sufficiency, which corresponded to 3858 kg h^{-1} for alternative 1 (named split fraction A, which was 64.3% of the total input) and 4212 kg h^{-1} for alternative 2 (split fraction B of 70.2%). In addition, to provide a comparison of both alternatives with the same mass feed rate for mannose production, a variant of alternative 1 – named alternative 1B – was simulated with the same feedstock fraction for combustion as that of alternative 2, which thus generated an electricity surplus sold to the grid (1.61 MW). Table 5 displays the main simulation results, including the feedstock distribution for combustion and biochemical processing (polyphenols, mannose and MOS production) and the resulting product flows.

Alternatives 1 and 1B recover 53% of açaí seeds' mannose potential as powdered mannose, in addition to 23% mannose syrup, achieving a mannose yield of 76% (Table 5), which is lower than the acid hydrolysis experimental yield ($Y_{1/0}$ of 82.5%) due to the assumed losses from purification processes. The proportion of mannose recovered in powder and syrup form (2.3 : 1, dry basis) is higher than in our previous work[5] (1.5 : 1) due to the incorporation of mannose syrup recycling to the evaporator, which enables increased high-purity crystal product formation. Powdered mannose has a higher purity and price (US$ 10 per kg) compared to mannose syrup (US$ 2 per kg dry weight);[5] nevertheless, its production increases the process energy requirements for cooling a larger crystallizer feed and for distilling the resulting mother liquor.

In alternative 2, a higher mannose yield of 81% is achieved in the overall process due to the sequential steps of acid and enzymatic hydrolysis. However, this approach generates a higher hydrolysate flow entering the mannose and MOS evaporator systems, significantly increasing the process heating demands and thus requiring a larger biomass feed rate for combustion (Table 5), which is in accordance with the results obtained for a sequential H$_2$SO$_4$-catalyzed hydrolysis followed by enzymatic hydrolysis process.[5] This explains why the sequential approach results in a lower absolute production rate of mannose (614 kg h^{-1} in powder form) when compared to alternative 1 (686 kg h^{-1}), despite the higher total mannose yield.

Internal demands of power, low pressure steam (LPS, 125 °C) and high pressure steam (HPS, 200 °C) in the three process alternatives are shown in Fig. 5. While HPS is used only in the acid hydrolysis reactor (S-300), LPS contributes to more than 90% of the heating demand as it is required in evaporator systems for the concentration of polyphenols, mannose and MOS (S-200, S-500 and S-600, respectively), and in distillation columns for oxalic acid (S-300) and mannose syrup (S-500) purification. The internal thermal energy demand of alternative 1 amounted to 17.5 MW$_t$, equivalent to 29.4 MJ kg^{-1} açaí seeds fed to biochemical processing, while alternative 2 required 18.2 MW$_t$, or 36.7 MJ kg^{-1} seeds. In addition, alternatives 1 and 2 required 1.1 MW$_e$ and 1.3 MW$_e$
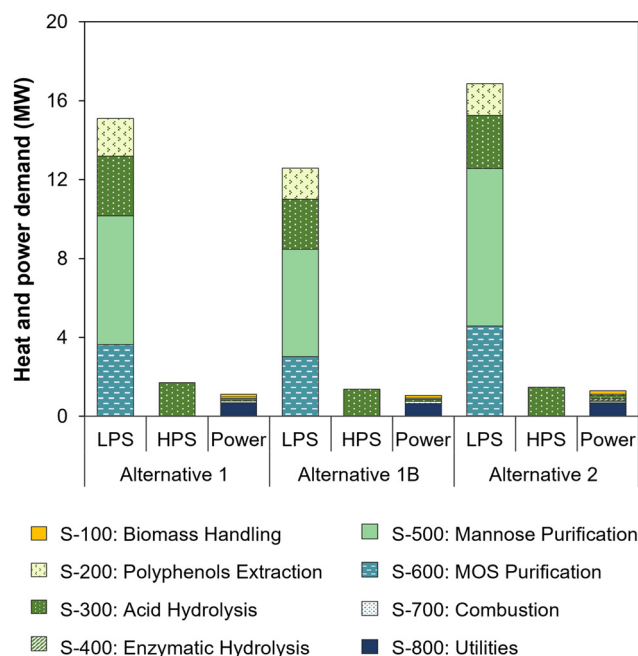
Fig. 5 Thermal and electric energy demands of process alternatives. Heating demand is shown for low pressure steam (LPS, 125 °C) and high pressure steam (HPS, 200 °C).

of electricity, which was mainly used in the cooling tower and chiller of the cold utilities section (S-800). Both thermal and electric energy demands of the process alternatives were internally met by heat and power cogeneration from seed combustion.

The specific heat demands of both alternatives were considerably higher than in our previous simulation of oxalic acid hydrolysis (16.1 MJ kg^{-1})[5] mainly due to the larger hydrolysate flow entering S-500 as a result of dilution (3 times) in the oxalic acid chromatography system. Hence, significant process improvements could be achieved by reducing the eluent flow required for sugar desorption from the chromatography resin. A potential solution may include the removal of the adsorbed sugars under vacuum, which has been reported to reduce the eluent flow by 5 times.[84] The use of weak base anion exchange resins could also be investigated, as they selectively retain organic acids while sugars pass through the column without significant dilution.[85] This approach was not considered in this work, because it would require a strong acid solution to elute the retained organic acid, followed by resin regeneration with a base, which would consume significant amounts of acids and bases and complicate further purification of oxalic acid. Another alternative could involve oxalic acid crystalliza-

tion after hydrolysate concentration, given the low solubility of oxalic acid at low temperature (6 g per 100 g water at 10 °C).[86] This process was successfully applied to a xylose-rich hydroly-sate, resulting in 85% recovery of oxalic acid after crystalliza-tion at 4 °C for 15 h.[87] Nevertheless, operation at such a low temperature would require a higher power demand in the chiller system, and an in-depth comparison of oxalic acid recovery strategies is beyond the scope of this work.

Despite the high thermal energy requirement resulting from oxalic acid recovery, the specific heat demand of alterna-tive 1 was equal to that of a process employing sequential sul-furic acid and enzymatic hydrolysis (29.4 MJ kg^{-1} açaí seeds), as reported earlier.[5] This indicates that the single-step oxalic acid hydrolysis process has a superior environmental perform-ance as it uses a catalyst with lower toxicity and achieves a comparable specific heat demand while also carrying out an extra step for oxalic acid recovery, which entails additional environmental benefits by avoiding the use of a base and the generation of salt waste.

3.5.2 Economic performance of process alternatives. The economic performance of the simulated processes was assessed, and results are shown in Fig. 6. Alternative 1 displays the best cost-efficiency due to lower capital and operational
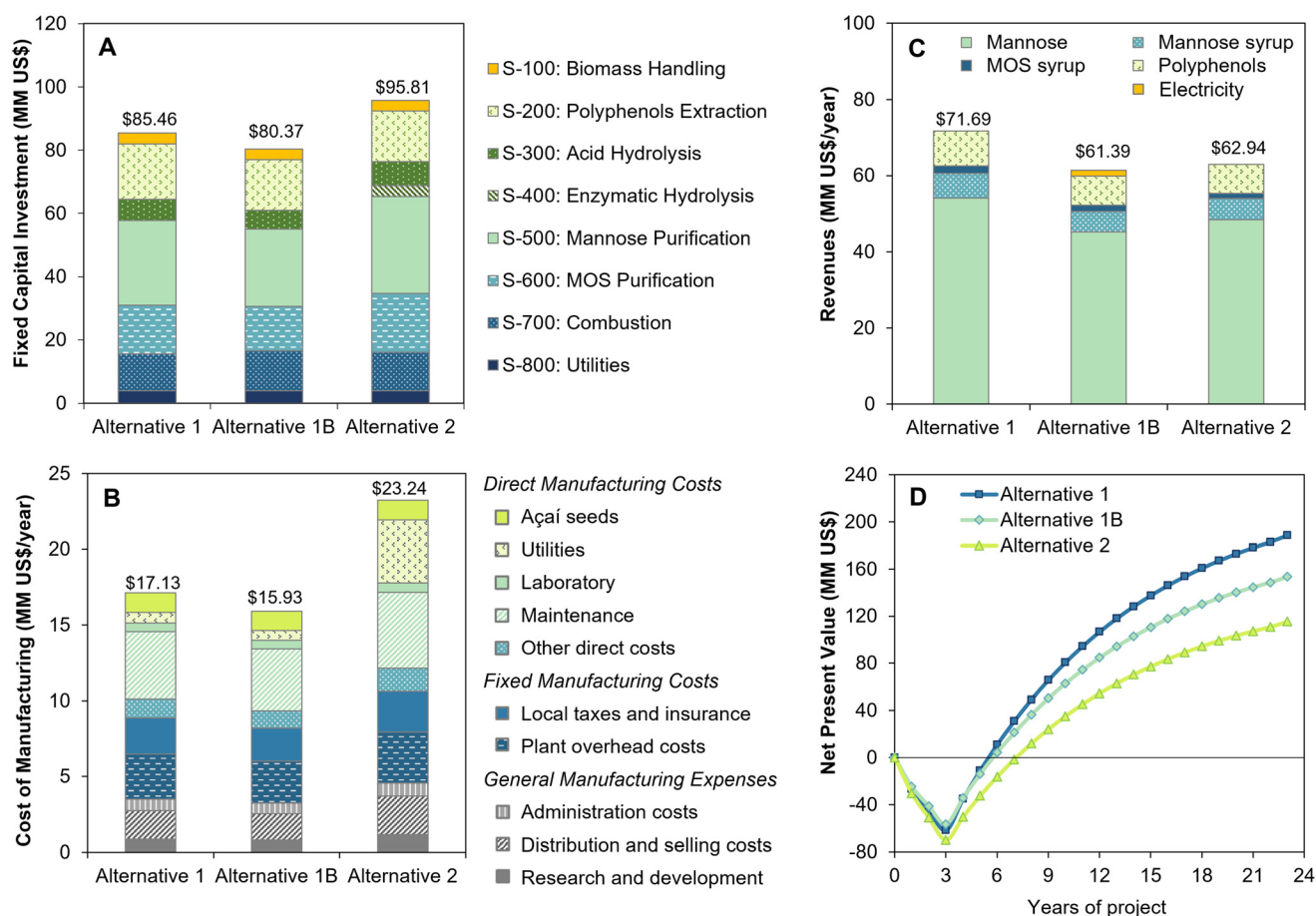
Fig. 6 Techno-economic results of biorefinery alternatives for açaí seed processing: (a) fixed capital investment, (b) cost of manufacturing, (c) rev-enues, and (d) net present value.

costs in comparison with alternative 2, along with higher revenues. Fig. 6a reveals that the fixed capital investment (FCI) of alternative 2 is 19% higher than that of alternative 1B (which has the same raw material feed distribution for biochemical processing and combustion), with the main contribution arising from S-500 and S-600 due to the larger capacity of mannose and MOS evaporators. In addition, the enzymatic hydrolysis section (S-400) adds US$ 3.46 MM to the FCI, while the larger acid hydrolysis reactor, required for a residence time of 65 min in alternative 2, increases the fixed investment of S-300 by 27% in comparison with alternative 1B. Additionally, the annual operational costs of alternative 2 are 46% higher than that of alternative 1B due to the high cost of enzymes (US$ 3.46 MM per year) and the higher investment for this alternative, which contributes to increased maintenance costs, fixed costs and general expenses (Fig. 6b). The revenues of alternative 1 (US$ 71.69 MM per year) are also higher than in alternative 2 (US$ 62.94 MM per year) due to the higher feedstock feed for biochemical processing (Fig. 6c).

Overall, the 2-step oxalic acid and enzymatic hydrolysis process displays similar disadvantages to those previously observed for sequential sulfuric acid and enzymatic hydrolysis.[5] Although the higher yield in oxalic acid hydrolysis reduced the enzyme consumption and costs compared to the sulfuric acid process, the additional oxalic acid recovery and MOS coproduction steps significantly increased the biorefinery capital investment and internal heat demand. This lowers the raw material feed rate for mannose production (1788 kg h^{-1} in alternative 2, as opposed to 2000 kg h^{-1} in the sulfuric acid process[5]), thus leading to an inferior economic performance, with an 18% reduction in NPV (US$ 117 MM *versus* US$ 143 MM[5]). Furthermore, when compared to the one-step oxalic acid process, the second step of enzymatic hydrolysis generates a significant increase in hydrolysate flow due to its lower solid loading (20% as opposed to 30% in acid hydrolysis), leading to higher capital and operational costs for purification. Therefore, the one-step dilute oxalic acid process is shown to be more advantageous, resulting in the highest NPV of US$ 188 MM after 20 years of operation and the fastest payback period of 2.5 years after process startup (Fig. 6d), with an IRR of 35.9%.

The economic performance of the one-step oxalic acid process was slightly improved compared to our previous study, where a NPV of US$ 137 MM was reached with a payback period of 2.7 years and an IRR of 34.8%.[5] The increase of 37% in the final NPV can be mainly attributed to 29% increase in revenues (from US$ 55.4 MM[5] to US$ 71.7 MM) due to the improved powdered mannose recovery and to MOS sales as a new coproduct. Nevertheless, a significantly higher FCI (US$ 73.9 MM is alternative 1, as opposed to US$ 57.7 MM[5]) was required for oxalic acid recycling and MOS coproduction, which balanced out the gains in revenues in the short term, leading to a similar economic performance with regard to the IRR and payback period.

To the best of our knowledge, no other economic studies have been made on mannose production from plant biomass containing linear mannan. Besides, there are no reports on the economic performance of commercial mannose production processes from yeast alpha-mannans or plant-derived glucomannans and galactomannans. Méndez *et al.* recently performed a techno-economic assessment of mannose production from softwood pulping side streams that were rich in galactoglucomannan (with a mannose : glucose : galactose ratio of 3 : 1 : 0.6). The study revealed that mannose – being the most valuable sugar – had a critical impact on the economic viability of the overall process, with a threshold selling price of €11.84 kg^{-1} (*i.e.*, the minimum selling price at which the process remains economically viable). In the açaí seed biorefineries evaluated herein, mannose is also the most valuable product, but the high mannan content of açaí seeds enables a much more competitive selling price, with a corresponding powdered mannose threshold price of US$ 1.86 per kg in alternative 1 if all other coproducts retain their original prices. Therefore, this work demonstrates the high economic potential of valorizing abundant and underexplored açaí seeds into mannose, increasing the market availability and enabling further applications of this rare sugar.

3.6 Environmental aspects of the processes

Besides the economic advantages over the sequential sulfuric acid and enzymatic hydrolysis process, the one-step oxalic acid hydrolysis process presented herein displays significant improvements in environmental performance. This new process replaces the highly toxic sulfuric acid (rat oral median lethal dose LD$_{50}$ of 2140 mg kg^{-1})[88] with oxalic acid, a less hazardous dicarboxylic acid (rat oral LD$_{50}$ of 7500 mg kg^{-1})[88] with a 10-times lower impact on aquatic toxicity (fathead minnow median lethal concentration of 294 mg L^{-1} as opposed to 25 mg L^{-1} for sulfuric acid).[88] Indeed, the aquatic toxicity potential of waste streams from açaí seed processing without acid recycling has been shown to significantly decrease when using oxalic acid instead of sulfuric acid.[5]

In addition to improved safety over sulfuric acid, another process-related advantage of oxalic acid-catalyzed hydrolysis arises from the coproduction of MOS. In this study, process simulations evaluated MOS recovery together with other monosaccharides, which were previously considered as a waste stream in the sulfuric acid process.[5] This MOS-rich syrup is purified for feed applications, reducing the biochemical oxygen demand of the aqueous waste stream resulting from such a purification process while generating a new coproduct for the biorefinery.

Nevertheless, despite being widely considered as a safer and greener alternative to sulfuric acid,[22–24] it is relevant to consider the indirect impacts of oxalic acid consumption, which are often overlooked in the literature. Currently, oxalic acid is largely produced *via* catalytic oxidation of ethylene glycol or propylene with nitric acid,[30] which are normally petrochemical products, where the latter pathway is reported to consume 1.2 kg of HNO$_3$ per kilogram of oxalic acid dihydrate produced, while the former does not involve large consumption of acids but is challenged by the high cost of the raw

material.[89] Biomass is also commercially used as a raw material, with carbohydrates being oxidized with HNO_3, usually in a solution of approximately 50% H_2SO_4 at around 70 °C, in the presence of a mixed catalyst of vanadium pentoxide and iron(III) sulfate.[89,90] The method is not fully environmentally advantageous, as, despite the renewable feedstock, it generates greater NO_x emissions, consumes HNO_3 and H_2SO_4, and suffers from low yields of ~65%.[30,89] A commercially available and more efficient alternative (dialkyl oxalate route) is to employ oxidative CO coupling in the presence of an alcohol, which is known to provide high yields.[30] Although it requires a small input of HNO_3 and generates nitrogen oxide, the impact can be substantially mitigated.[91] Alternatively, more recent and promising technology, already shown to be economically feasible[92] but still only developed at the level of pilot demonstration,[30] prescribes the electrochemical reduction of CO_2 to formate, followed by a formate to oxalate coupling reaction, and oxalate acidification by electrodialysis,[93] which shows potential for low-emission and sustainable production if powered by renewable electricity. Schuler *et al.* discussed the sustainability aspects of these and other oxalic acid production pathways in detail;[30] however, comprehensive life cycle assessments of such processes are still missing.

In this context, to ensure superiority in environmental performance of oxalic acid mediated processes over sulfuric acid use, it is relevant to consider the source of oxalic acid and to reduce its consumption in the process. Hence, in this study, the recovery and recycling of oxalic acid were evaluated *via* process simulation, aiming to reduce its consumption and production-related impacts. Moreover, acid recycling avoids the addition of a base for hydrolysate neutralization and the generation of an oxalate salt waste stream that is harmful and toxic to terrestrial life if not adequately managed and disposed of.[5]

However, a relevant drawback of the process is its thermal energy requirement, primarily arising from the concentration steps for mannose and MOS following acid hydrolysate dilution during oxalic acid separation. Therefore, future research efforts should aim to demonstrate the separation performance of oxalic acid from the mannose-rich hydrolysate, while minimizing eluent flow and hydrolysate dilution. Nonetheless, process simulations demonstrated a specific thermal energy demand of 29.4 MJ kg^{-1} of processed açaí seeds, analogous to that of a sequential sulfuric acid–enzyme hydrolysis process.[5] Moreover, this internal energy demand is supplied by heat recovery from seed combustion, thus relying on renewable energy from agroindustrial waste.

Finally, when considering the açaí value chain, the proposed biorefinery could alleviate the current environmental problem of inadequate disposal and accumulation of açaí seeds, besides adding value to this residue and leveraging local sustainable development. Therefore, the high-yield one-step hydrolysis process developed herein, alongside an efficient and yet-to-be-tested separation method for mannose and oxalic acid, is demonstrated as a viable and sustainable route to açaí seed valorization, which could contribute to a circular bioeconomy in the Amazon region.

4. Conclusion

This work developed a high-yield single-step process employing dilute oxalic acid to produce mannose and MOS from açaí seeds, an abundant and underexplored agroindustrial waste. Mannose production was optimized considering the effects of hydrolysis temperature, time, and acid concentration, achieving a mannose yield of 83% – the highest ever reported for a one-step hydrolysis of recalcitrant linear mannan using an organic acid. In addition to mannose, MOS were coproduced in 9.6% yield, reaching a combined yield of 92% for both products. Economic viability was demonstrated by simulation on an industrial scale, achieving high profitability with a net present value of US$ 188 million and a payback period of 2.5 years after startup. This process also offers significant safety and environmental benefits compared to a previous 2-step method using sulfuric acid and enzymatic hydrolysis. Besides using an acid with lower toxicity, process simulations indicate a comparable specific thermal energy consumption while considering an additional step for oxalic acid recovery, which avoids the use of a base for neutralization and the generation of salt waste. Therefore, this study demonstrates an efficient and economically viable process for mannose production that aligns with the green chemistry principles, including the use of renewable raw materials and less toxic chemicals, improving safety, performing efficient catalysis, and reducing waste.

Author contributions

F. T. A. Jorge: investigation, formal analysis, visualization, writing – original draft, writing – review & editing. I. S. Miguez: methodology, writing – review & editing. G. V. Brigagão: validation, supervision, writing – review & editing. A. S. Silva: conceptualization, writing – review & editing, validation, resources, supervision, project administration, funding acquisition.

Data availability

All data generated or analyzed during this study are included in this article. Any additional information is available from the corresponding author on request.

Conflicts of interest

F. T. A. Jorge, I. S. Miguez., and A. S. Silva are inventors of a patent issued to the Instituto Nacional de Tecnologia (BR102023005989-9) concerning the one-step oxalic acid hydrolysis process of açaí seeds for mannose production described in this paper. The authors declare no other financial or non-financial competing interests.

Acknowledgements

References

1 E. de Jong, H. Stichnothe, G. Bell and H. Jørgensen, *Bio-Based Chemicals: a 2020 Update*, IEA Bioenergy – Task42 Biorefinery, 2020.

2 R. R. Philippini, S. E. Martiniano, A. P. Ingle, P. R. F. Marcelino, G. M. Silva, F. G. Barbosa, J. C. dos Santos and S. S. da Silva, *Front. Energy Res.*, 2020, **8**, 1–23.

3 R. B. Melati, F. L. Shimizu, G. Oliveira, F. C. Pagnocca, W. de Souza, C. Sant'Anna and M. Brienzo, *Bioenergy Res.*, 2019, **12**, 1–20.

4 R. Zhang, H. Gao, Y. Wang, B. He, J. Lu, W. Zhu, L. Peng and Y. Wang, *Bioresour. Technol.*, 2023, **369**, 128315.

5 F. T. A. Jorge, A. S. da Silva and G. V. Brigagão, *Biomass Convers. Biorefin.*, 2024, **14**, 3739–3752.

6 J. R. Barbosa and R. N. de Carvalho Junior, *Trends Food Sci. Technol.*, 2022, **124**, 86–95.

7 S. F. D. S. Chaves, R. M. Alves and L. A. D. S. Dias, *Crop Breed. Appl. Biotechnol.*, 2021, **21**, 1–13.

8 IBGE, Tabela 5457 - Área plantada ou destinada à colheita, área colhida, quantidade produzida, rendimento médio e valor da produção das lavouras temporárias e permanentes, **https://sidra.ibge.gov.br/tabela/5457**, (accessed 21 February 2024).

9 J. D. C. Pessoa, M. Arduin, M. A. Martins and J. E. U. de Carvalho, *Braz. Arch. Biol. Technol.*, 2010, **53**, 1451–1460.

10 G. R. Martins, M. M. G. Mattos, F. M. Nascimento, F. L. Brum, R. Mohana-Borges, N. G. Figueiredo, D. F. M. Neto, G. B. Domont, F. C. S. Nogueira, F. D. A. de P. Campos and A. S. da Silva, *J. Agric. Food Chem.*, 2022, **70**, 16218–16228.

11 G. R. Martins, F. R. L. do Amaral, F. L. Brum, R. Mohana-Borges, S. S. T. de Moura, F. A. Ferreira, L. S. Sangenito, A. L. S. Santos, N. G. Figueiredo and A. S. da Silva, *Lwt*, 2020, **132**, 109830.

12 P. S. Melo, M. M. Selani, R. H. Gonçalves, J. de O. Paulino, A. P. Massarioli and S. M. de Alencar, *Ind. Crops Prod.*, 2021, **161**, 113204.

13 A. F. Monteiro, I. S. Miguez, J. P. R. B. Silva and A. S. da Silva, *Sci. Rep.*, 2019, **9**, 1–12.

14 M. K. D. Rambo, F. L. Schmidt and M. M. C. Ferreira, *Talanta*, 2015, **144**, 696–703.

15 P. Wang, Y. Zheng, Y. Li, J. Shen, M. Dan and D. Wang, *Curr. Res. Food Sci.*, 2022, **5**, 49–56.

16 X. Hu, Y. Shi, P. Zhang, M. Miao, T. Zhang and B. Jiang, *Compr. Rev. Food Sci. Food Saf.*, 2016, **15**, 773–785.

17 M. H. L. Sandoval, C. M. Caixeta and N. M. Ribeiro, *Surg. Cosmet. Dermatol.*, 2015, **7**, 37–44.

18 P. Spring, C. Wenk, A. Connolly and A. Kiers, *J. Appl. Anim. Nutr.*, 2015, **3**, 1–11.

19 N. Kango, U. K. Jana, R. Choukade and S. Nath, *Curr. Opin. Food Sci.*, 2022, **47**, 100883.

20 Q. A. Nguyen, E. J. Cho, D. S. Lee and H. J. Bae, *Bioresour. Technol.*, 2019, **272**, 209–216.

21 M. Hara, Y. Kita, R. Haige and H. Yamada, *US Pat*, 20210164064A1, 2021.

22 B. Liu, L. Liu, B. Deng, C. Huang, J. Zhu, L. Liang, X. He, Y. Wei, C. Qin, C. Liang, S. Liu and S. Yao, *Int. J. Biol. Macromol.*, 2022, **222**, 1400–1413.

23 J. W. Lee and T. W. Jeffries, *Bioresour. Technol.*, 2011, **102**, 5884–5890.

24 Y. Yan, C. Zhang, Q. Lin, X. Wang, B. Cheng, H. Li and J. Ren, *Molecules*, 2018, **23**, 862.

25 H. Kayser, F. Rodríguez-Ropero, W. Leitner, M. Fioroni and P. D. de María, *RSC Adv.*, 2013, **3**, 9273–9278.

26 J. W. Lee, R. C. L. B. Rodrigues, H. J. Kim, I. G. Choi and T. W. Jeffries, *Bioresour. Technol.*, 2010, **101**, 4379–4385.

27 M. Mottakin, V. Selvanathan, S. Mandol, M. M. Hossen, M. Nurunnabi, J. Bin Haider, M. Hasan, K. Althubeiti, D. K. Sarkar, M. Shahinuzzaman, H. Abdullah and M. Akhtaruzzaman, *J. Cleaner Prod.*, 2022, **339**, 130704.

28 G. J. G. Ruijter, P. J. I. van de Vondervoort and J. Visser, *Microbiology*, 1999, **145**, 2569–2576.

29 E. Betiku, H. A. Emeko and B. O. Solomon, *Heliyon*, 2016, **2**, e00082.

30 E. Schuler, M. Demetriou, N. R. Shiju and G. J. M. Gruter, *ChemSusChem*, 2021, **14**, 3636–3664.

31 Q. Qing, M. Huang, Y. He, L. Wang and Y. Zhang, *Appl. Biochem. Biotechnol.*, 2015, **177**, 1493–1507.

32 D. Scordia, S. L. Cosentino and T. W. Jeffries, *Ind. Crops Prod.*, 2013, **49**, 392–399.

33 P. Amnuaycheewa, R. Hengaroonprasan, K. Rattanaporn, S. Kirdponpattara, K. Cheenkachorn and M. Sriariyanun, *Ind. Crops Prod.*, 2016, **87**, 247–254.

34 Y. Tao, Y. Zhao, Y. Sheng, L. Ruan, W. Ge, H. Lin, Q. Qing, Y. Zhang and L. Wang, *Int. J. Biol. Macromol.*, 2024, **265**, 130721.

35 T. J. Bondancia, J. De Aguiar, G. Batista, A. J. G. Cruz, J. M. Marconcini, L. H. C. Mattoso and C. S. Farinas, *Ind. Eng. Chem. Res.*, 2020, **59**, 11505–11516.

36 S. E. AbdElhafez, T. Taha, A. E. Mansy, E. El-Desouky, M. A. Abu-Saied, K. Eltaher, A. Hamdy, G. El Fawal, A. Gamal, A. M. Hashim, A. S. Elgharbawy, M. M. A. El-Latif, H. Hamad and R. M. Ali, *Energies*, 2022, **15**, 6131.

37 R. Cao, X. Liu, J. Guo and Y. Xu, *Biotechnol. Biofuels*, 2021, **14**, 1–8.

38 J. Viell, A. Harwardt, J. Seiler and W. Marquardt, *Bioresour. Technol.*, 2013, **150**, 89–97.

39 A. Sluiter, B. Hames, R. Ruiz, C. Scarlata, J. Sluiter and D. Templeton, *Determination of Sugars, Byproducts, and Degradation Products in Liquid Fraction Process Samples*, Laboratory Analytical Procedure (LAP), Golden, CO, 2006.

40 H. L. Chum, D. K. Johnson and S. K. Black, *Ind. Eng. Chem. Res.*, 1990, **29**, 156–162.

41 A. Sluiter, B. Hames, R. Ruiz, C. Scarlata, J. Sluiter, D. Templeton and D. Crocker, Determination of structural carbohydrates and lignin in Biomass, *Laboratory Analytical Procedure (LAP)*, Golden, CO, 2012.

42 R. J. Wooley and V. Putsche, Development of an ASPEN PLUS Physical Property Database for Biofuels Components, Golden, CO, 1996.

43 Y. Xie, D. Phelps, C. H. Lee, M. Sedlak, N. Ho and N. H. L. Wang, *Ind. Eng. Chem. Res.*, 2005, **44**, 6816–6823.

44 R. M. Springfield and R. D. Hester, *Sep. Sci. Technol.*, 2001, **36**, 911–930.

45 A. R. Oroskar, N. S. Sudharsan, P. A. Oroskar and O. M. Kulkarni, *US Pat*, 9163050B2, 2015.

46 I. Mueller, A. Seidel-Morgenstern and C. Hamel, *Sep. Purif. Technol.*, 2021, **271**, 1–11.

47 K. Vaňková and M. Polakovič, *Chem. Eng. Technol.*, 2012, **35**, 161–168.

48 Z. Lin, J. Wang, V. Nikolakis and M. Ierapetritou, *Comput. Chem. Eng.*, 2017, **102**, 258–267.

49 T. Sainio, I. Turku and J. Heinonen, *Bioresour. Technol.*, 2011, **102**, 6048–6057.

50 R. Turton, J. A. Shaeiwitz, D. Bhattacharyya and W. B. Whiting, *Analysis, Synthesis, and Design of Chemical Processes*, Pearson Education, Boston, MA, USA, 5th edn, 2018.

51 M. Tsagkari, J. L. Couturier, A. Kokossis and J. L. Dubois, *ChemSusChem*, 2016, **9**, 2284–2297.

52 P. Christensen and L. R. Dysert, AACE International Recommended Practice No. 18R-97: Cost estimate classification system - as applied in engineering, procurement, and construction for the process industries, 2005.

53 Trading Economics, Brazil Real Average Monthly Income in Manufacturing, **https://tradingeconomics.com/brazil/wages-in-manufacturing**, (accessed 20 September 2023).

54 Zauba, Analysis of Import of: mannose syrup, **https://www.zauba.com/importanalysis-mannose+syrup-report.html**, (accessed 16 February 2024).

55 ANP, Anuário Estatístico 2022 - Dados Abertos, **https://www.gov.br/anp/pt-br/centrais-de-conteudo/dados-abertos/anuario-estatistico-2022**, (accessed 20 September 2023).

56 D. R. Woods, *Rules of Thumb in Engineering Practice*, WILEY-VCH Verlag GmbH & Co. KGaA, Weinheim, 2007, vol. 53.

57 Alibaba, Fructooligosaccharides syrup FOS Syrup Fructo-oligosaccharide syrup, **https://www.alibaba.com/product-detail/Fructooligosaccharides-syrup-FOS-Syrup-Fructo-oligosaccharide_62375990672.html?spm=a2700.galleryofferlist.normal_offer.d_title.41a01391JPhu21**, (accessed 16 February 2024).

58 Alibaba, Top Quality IMO 900 isomalto-oligosaccharide Syrup, **https://www.alibaba.com/product-detail/Top-Quality-IMO-900-isomalto-oligosaccharide_1600321251587.html?spm=a2700.galleryofferlist.normal_offer.d_title.41a01391JPhu21**, (accessed 16 February 2024).

59 A. S. da Silva, A. F. Monteiro, J. P. R. B. da Silva and I. S. Miguez, *BR Pat*. 102018067282B1, 2018.

60 W. Igreja, L. da Silva Martins, R. de Almeida, J. de Oliveira, A. Lopes and R. Chisté, *Molecules*, 2023, **28**, 6661.

61 Y. Lu and N. S. Mosier, *Biotechnol. Prog.*, 2007, **23**, 116–123.

62 M. Faustino, J. Durão, C. F. Pereira, M. E. Pintado and A. P. Carvalho, *Carbohydr. Polym.*, 2021, **272**, 118467.

63 M. Chua, K. Chan, T. J. Hocking, P. A. Williams, C. J. Perry and T. C. Baldwin, *Carbohydr. Polym.*, 2012, **87**, 2202–2210.

64 F. Rashid, S. Hussain and Z. Ahmed, *Carbohydr. Polym.*, 2018, **180**, 88–95.

65 V. D. Prajapati, G. K. Jani, N. G. Moradiya, N. P. Randeria, B. J. Nagar, N. N. Naikwadi and B. C. Variya, *Int. J. Biol. Macromol.*, 2013, **60**, 83–92.

66 B. T. Kusema, T. Tönnov, P. Mäki-Arvela, T. Salmi, S. Willför, B. Holmbom and D. Y. Murzin, *Catal. Sci. Technol.*, 2013, **3**, 116–122.

67 C. Xu, A. Pranovich, L. Vähäsalo, J. Hemming, B. Holmbom, H. A. Schols and S. Willför, *J. Agric. Food Chem.*, 2008, **56**, 2429–2435.

68 M. Zhang, X. L. Chen, Z. H. Zhang, C. Y. Sun, L. L. Chen, H. L. He, B. C. Zhou and Y. Z. Zhang, *Appl. Microbiol. Biotechnol.*, 2009, **83**, 865–873.

69 B. Gómez, B. Míguez, R. Yáñez and J. L. Alonso, *J. Agric. Food Chem.*, 2017, **65**, 2019–2031.

70 T. Miyazawa and T. Funazukuri, *Carbohydr. Res.*, 2006, **341**, 870–877.

71 E. J. Cho, Y. G. Lee, Y. Song, D.-T. Nguyen and H.-J. Bae, *Bioresour. Technol.*, 2022, **346**, 126618.

72 J. Gu, W. Pei, S. Tang, F. Yan, Z. Peng, C. Huang, J. Yang and Q. Yong, *Int. J. Biol. Macromol.*, 2020, **149**, 572–580.

73 S. L. Murillo-Franco, J. D. Galvis-Nieto and C. E. Orrego, *Processes*, 2024, **12**, 847.

74 H. Zhang, Y. Xu and S. Yu, *Bioresour. Technol.*, 2017, **234**, 343–349.

75 Q. Lin, H. Li, J. Ren, A. Deng, W. Li, C. Liu and R. Sun, *Carbohydr. Polym.*, 2017, **157**, 214–225.

76 Y. Lu and N. S. Mosier, *Biotechnol. Bioeng.*, 2008, **101**, 1170–1181.

77 B. Danon, G. Marcotullio and W. De Jong, *Green Chem.*, 2014, **16**, 39–54.

78 A. M. J. Kootstra, N. S. Mosier, E. L. Scott, H. H. Beeftink and J. P. M. Sanders, *Biochem. Eng. J.*, 2009, **43**, 92–97.

79 Y. Kim, T. Kreke and M. R. Ladisch, *AIChE J.*, 2013, **59**, 188–199.

80 A. Avci, B. C. Saha, B. S. Dien, G. J. Kennedy and M. A. Cotta, *Bioresour. Technol.*, 2013, **130**, 603–612.

81 G. R. Martins, D. Guedes, U. L. Marques, M. D. S. de Paula, P. de Oliveira, M. T. S. Lutterbach, L. Y. Reznik, E. F. C. Sérvulo, C. S. Alviano, A. J. R. da Silva and D. S. Alviano, *Molecules*, 2021, **26**, 3433.

82 R. O. Araujo, F. C. P. Ribeiro, V. O. Santos, V. M. R. Lima, J. L. Santos, J. E. S. Vilaça, J. S. Chaar, N. P. S. Falcão, A. M. Pohlit and L. K. C. de Souza, *BioEnergy Res.*, 2022, **15**, 834–849.

83 Y. Itai, R. Santos, M. Branquinho, I. Malico, G. F. Ghesti and A. M. Brasil, *Renewable Energy*, 2014, **66**, 662–669.

84 R. D. Hester, G. E. Farina and S. Nangueri, *US Pat*, 5407580A, 1995.

85 C. S. López-Garzón and A. J. J. Straathof, *Biotechnol. Adv.*, 2014, **32**, 873–904.

86 C. Srinivasakannan, R. Vasanthakumar, K. Iyappan and P. G. Rao, *Chem. Biochem. Eng. Q.*, 2002, **16**, 125–129.

87 T. vom Stein, P. M. Grande, H. Kayser, F. Sibilla, W. Leitner and P. D. de María, *Green Chem.*, 2011, **13**, 1772–1777.

88 R. J. Lewis, *Sax's Dangerous Properties of Industrial Materials*, John Wiley & Sons, Inc., 11th edn, 2004.

89 W. Riemenschneider and M. Tanifuji, *Ullmann's Encyclopedia of Industrial Chemistry*, Wiley, 2011.

90 H. Sawada and T. Murakami, *Kirk-Othmer Encyclopedia of Chemical Technology*, John Wiley & Sons, Inc., 2000.

91 J. Zhu, L. Hao, Y. Sun, B. Zhang, W. Bai and H. Wei, *Comput. Chem. Eng.*, 2018, **115**, 198–212.

92 V. Boor, J. E. B. M. Frijns, E. Perez-Gallent, E. Giling, A. T. Laitinen, E. L. V. Goetheer, L. J. P. van den Broeke, R. Kortlever, W. de Jong, O. A. Moultos, T. J. H. Vlugt and M. Ramdin, *Ind. Eng. Chem. Res.*, 2022, **61**, 14837–14846.

93 E. Schuler, M. Morana, P. A. Ermolich, K. Lüschen, A. J. Greer, S. F. R. Taylor, C. Hardacre, N. R. Shiju and G. J. M. Gruter, *Green Chem.*, 2022, **24**, 8227–8258.